Advanced laboratory course

Measurement of matter-antimatter asymmetries with the LHCb experiment

Theodor Zies
theodor.zies@tu-dortmund.de

Can Toraman
can.toraman@tu-dortmund.de

Colloqium: 17.06.24

Hand-in: 08.07.2024

TU Dortmund – Physics department

Contents

1 Objective

During the Big Bang, equal amounts of matter and antimatter should have been created. However, our universe almost exclusively contains regular matter. This so-called matter-antimatter problem remains unsolved until today. It can partially be explained by the violation of the matter-antimatter (CP) symmetry in weak decays. This analysis uses data from weak B meson decays recorded at the LHCb experiment to quantify the CP asymmetry.

2 Theory

To understand how weak B meson decays at LHCb can be used to study CP violation, it is necessary to explain the origin of CP violation in the standard model (SM) of particle physics first. The following section gives a short overview about how CP violation was discovered and the way it is parameterized in the SM.

2.1 The CKM matrix and CP violation

In 1973, Kobayashi and Maskawa [2] completed the quark sector of the SM by introducing a third generation of quarks, the top (t) and bottom (b) quark. Thus in total, three up-type quarks (u, c, t) and three down-type quarks (d, s, b) exist in the SM. During weak processes, the quarks couple to the W and Z bosons in their weak eigenbasis. The weak eigenstates result from mixing the physical eigenstates of the quarks, this mixing is described by the CKM matrix:

$$\begin{pmatrix} d' \\ s' \\ b' \end{pmatrix} = \underbrace{\begin{pmatrix} V_{\mathrm{ud}} & V_{\mathrm{us}} & V_{\mathrm{ub}} \\ V_{\mathrm{cd}} & V_{\mathrm{cs}} & V_{\mathrm{cb}} \\ V_{\mathrm{td}} & V_{\mathrm{ts}} & V_{\mathrm{tb}} \end{pmatrix}}_{V_{\mathrm{CKM}}} \cdot \begin{pmatrix} d \\ s \\ b \end{pmatrix}.$$

Another way of interpreting this matrix is that each element quantifies how likely it is for a transition from one specific quark type to another to occur. The CKM matrix is a complex and unitary 3×3 matrix, which is why it has four free parameters. Three of these parameters are the previously mentioned quark mixing angles, however the fourth parameter is a complex phase δ. This phase describes the CP violation and is the main reason why the third generation of quarks was introduced. The CP is a short form for the charge (C) and parity (P) symmetry, which describes the fact that an antiparticle (regular particle with opposite charge and parity) is expected to behave exactly the same as its regular particle counterpart. In 1964, violation of this CP-symmetry in weak Kaon decays was observed and could not be described at first. The violation could finally explained through the implementation of the previously mentioned CP violation phase in 1973.
The CKM matrix elements have been experimentally measured and show a clear hierachy in respect to the different generations. A possible way of parameterizing the matrix is

the so-called Wolfenstein parameterization (at λ^3 order):

$$V_{\mathrm{CKM}} \simeq \begin{pmatrix} 1-\frac{1}{2}\lambda^2 & \lambda & A\lambda^3(\rho-\mathrm{i}\eta) \\ -\lambda & 1-\frac{1}{2}\lambda^2 & A\lambda^2 \\ A\lambda^3(1-\rho-\mathrm{i}\eta) & -A\lambda^2 & 1 \end{pmatrix}.$$

The complex CP violating phase is represented in the parameters ρ and η in this case. It is important to note that these parameters only appear in the matrix elements V_{ub} and V_{td} which will become important later.

2.2 CP violation in weak decays of B mesons

This analysis aims to study CP violation in weak B-meson decays. More specifically, decays of the B^+ meson and its CP counterpart B^- of the following form are considered:

$$B^+ \to h^+h^+h^-$$
$$B^- \to h^-h^-h^+$$

Without CP violation, one would expect to observe the same number of B^+ decays (N^+) as B^- decays (N^-). However, during the weak decay of the B meson consisting of a b and u quark, quark transitions of the form $b \to u$ can occur. The corresponding CKM matrix element V_{ub} is a complex number, as explained in the previous section. Consequently, the matrix element differs if a different CP variant of the decay is considered, due to the complex conjugation involved. In practice, the observed counts N^+ and N^- will be different and a CP asymmetry can be defined [3] as:

$$A_{\mathrm{CP}} = \frac{N^+ - N^-}{N^- + N^+}. \tag{1}$$

During the B decay, intermediate resonances contaning c quarks can occur due to e.g. quark transitions of the form $b \to c$. Examples for this are different D-mesons or charmonium ($c\bar{c}$) resonances. These resonances have to be removed, because the CP violation is much smaller in this case. The reason for this is the CKM matrix element V_{cb} that does not contain the CP violating parameters ρ and η (at the given order).

3 The LHCb detector

The large hadron collider (LHC) located at CERN near Geneva is the largest particle accelerator to date. Opposing proton beams are collided at four different interaction points with center of mass energies up to 13 TeV. Every interaction point houses one experiment, with each of them having a detector that is optimized for a different physics purpose. The four experiments are called ALICE, ATLAS, CMS and LHCb. The data used in this analysis is recorded at the LHCb detector. This detector is optimized for the study of b physics and measurements of CP violation parameters, which is exactly the type of physics present in the B meson decays that are analysed in this lab course.

The LHCb detector is a single-arm forward spectrometer, this particular design was chosen because the particles studied at LHCb are mainly produced with a strong boost in the forward direction. The polar anglular coverage reaches from 15 to 300 mrad [3]. A schematic view of the LHCb detector can be seen in Figure 1 at the status during the first data-taking period. Here, the z-axis is along the beam direction, the negative z-region is referred to as upstream, while the positive z-region is called downstream.

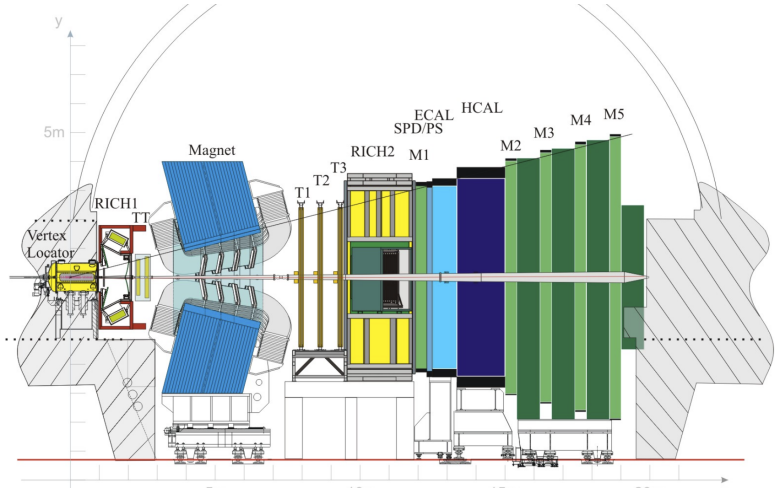

Figure 1: Cross-section of the LHCb detector, the following components are shown from left to right: The vertex locator (VELO), the Cherenkov detectors (RICH1,RICH2), the tracking system (TT and T1,T2,T3) including the magnet, the calorimeters (ECAL, HCAL) and the muon chambers (M1-M5).

The first component of the detector is the vertex locator (VELO), it is located directly at the interaction point. The VELO consits of multiple silicon strip detectors, meant to reconstruct the position of the proton-proton interaction, the primary vertex, and the decay location of the b hadron (secondary vertex). The B mesons typically have a flight path length of a few mm to cm and thus decay directly inside the VELO. The Ring Imaging Cherenkov (RICH) detectors 1 and 2 are used to calculate the velocity of transversing particles. This is archieved by measuring the diameter of light cones emitted by these particles due to the Cherenkov effect.
To obtain information about the particles momentum and charge, they are deflected by a dipole magnet with an integrated field strength of about 4 T m. Charged particles will then travel on a curved track. The tracking stations TT and T1-3 consit of large-area, four-layer silicon strip detectors as well as drift tubes. They measure the curved particle tracks and thus their radius can be determined. This allows it to calculate the momentum of the particle, while its charge is given by the direction of the particles deflection in the magnet. Combining the information about particle momentum, velocity and charge allows for particle identification (PID). Further downstream lies the calorimeter system, it is divided into the electromagnetic (ECAL) and hadronic (HCAL) calorimeters. The main purpose of the calorimeters is the measurement of the energy deposited by photons

and electrons in the ECAL and hadrons in the HCAL, respectively. Additionally the calorimeters also contribute to PID. The last main components are the five muon stations located at the end of the detector. Here, muons that traverse all other detector parts without much interaction can be measured.
While the proton proton collisions occur at a rate of 11 MHz, event storage is only possible with a rate of 3 kHz [3]. To reduce the number of events, only physically interesting events are selected via a trigger system consisting of a hardware and software implementation.

4 Analysis strategy

The data to be analysed was collected at LHCb in 2011 with a center of mass energy of 7 TeV at an integrated luminosity of $\approx 500\,\mathrm{pb}^{-1}$. A preselection has already been applied, significantly reducing background events that do not origin from the B meson decays. The data is split into 3.4 million events with upwards polarity of the dipole magnet and 5.1 million events with downwards polarity. Each event is of the type $B^{\pm} \to h^{+}h^{-}h^{\pm}$. Additionally, simulations of the decay $B^{\pm} \to K^{+}K^{-}K^{\pm}$ exist that only describe the decay into three Kaons. In contrast to the actual data, the simulations do not take intermediate resonances into account. The number of observables inside the dataset has already been reduced to a small set of essential variables.
As a first step, the distribution of individual variables is checked in the simulated data. The invariant mass of the B meson is calculated and histogrammed using the formula

$$m^2_{\mathrm{inv}} = P_{\mu}P^{\mu}\,, \tag{2}$$

with P_{μ} beeing the total four momentum of the decay products. In order to proceed in the same way with the actual data, the background that is present has to be reduced. A preselection is already applied, but additional requirements on PID have to be made. Signal candidates for the decay $B^{\pm} \to K^{+}K^{-}K^{\pm}$ are selected, while the selection efficiency can be checked using the availabe simulation. After the selection, the invariant mass of the B meson can again be calculated and compared with the previous result from the simulation. After a succesfull selection, the counts of signal candidates for the B^{+} and B^{-} decays are known and can be used to determine the CP asymmetry. Its uncertainty is given by:

$$\sigma_A = \sqrt{\frac{1-A^2}{N^{+}+N^{-}}}\,, \tag{3}$$

while the significance of the asymmetry can be calculated using

$$s(A) = \frac{A}{\sigma_A}\,. \tag{4}$$

A popular technique to visualize resonances in three-body decays are Dalitz plots. Here, two of the squared invariant masses from the combination of each two final state particles are usually plotted against each other. Any intermediate resonance will then be visible as a band in the plot, where the position and size of the band allow to infer on the mass

and width of the resonance. In the case of this analysis, the Dalitz plots are used to locate and remove charm resonances due to the low CP violation in this region.
Lastly, the Dalitz plots are used to determine local CP asymmetry. In this case, local refers to the fact that the asymmetry is calculated in a specific region of the phase space or a specic region in the Dalitz plot, respectively. In this manner, the areas with the most significant amount of CP asymmetry are determined and highlighted in the plot.

5 Analysis

Before working with the actual data, a simulation sample is used to familiarize oneself with the structure of the data. This simulation sample includes only $B^{\pm}$ candidates decaying into three Kaons. The distributions of the momenta belonging to the first Kaon are shown in Figure 2.

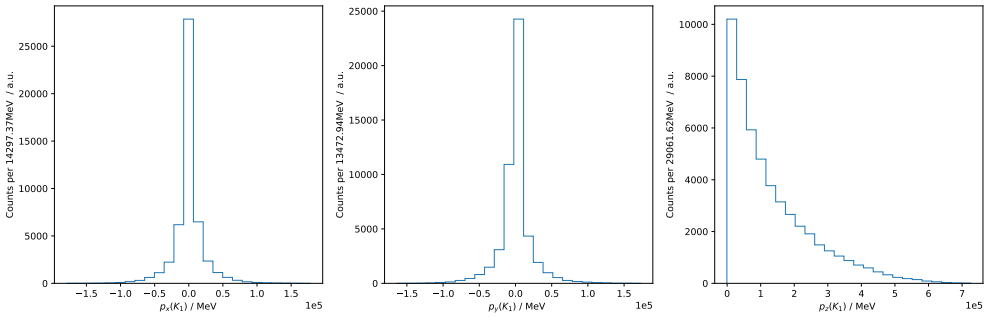

Figure 2: Momentum distributions of the fist Kaon.

From the momenta and the nominal mass of the Kaon $m(K^{\pm}) = (493.677 \pm 0.015)\,\mathrm{MeV}$ the energy carried by the Kaon is determined [1]. The energy distribution is shown in Figure 3

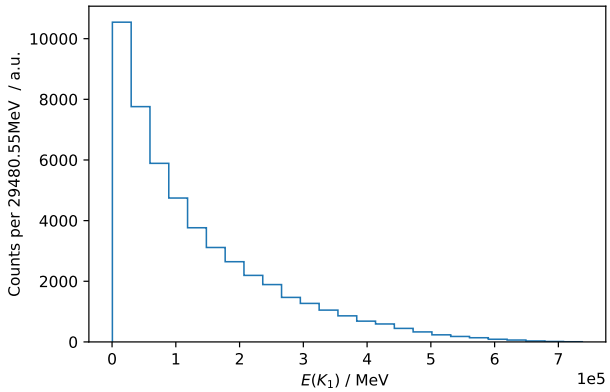

Figure 3: Histogram of the energy determined from the fist Kaons momenta.

Using the determined energy and momenta of the Kaons, the four momenta of the $B^{\pm}$ can be calculated. The four momenta are then used to determine the invariant mass of the $B^{\pm}$ according to (2). This distribution is not shown as the peak around the nominal mass $m(B^{\pm}) = (5279.41 \pm 0.07)\,\mathrm{MeV}$ is too narrow for histogramming [1].

Before working with the data sample, an additional requirement is placed on the `prob` variables to ensure the studied candidates originate from the $B^{\pm} \to K^{+}K^{-}K^{\pm}$ decay. This requirement is applied, because the data sample contains candidates from additional decays, e.g. including Pions. The values for the requirement on the candidate's determined probability are chosen as:

$$\texttt{H1\_probK} > 0.5 \tag{5}$$

$$\texttt{H1\_probPi} < 0.5 \tag{6}$$

The same steps explained for the simulation sample are then performed on the data sample to obtain the B-Mesons invariant mass distribution, shown in Figure 4.

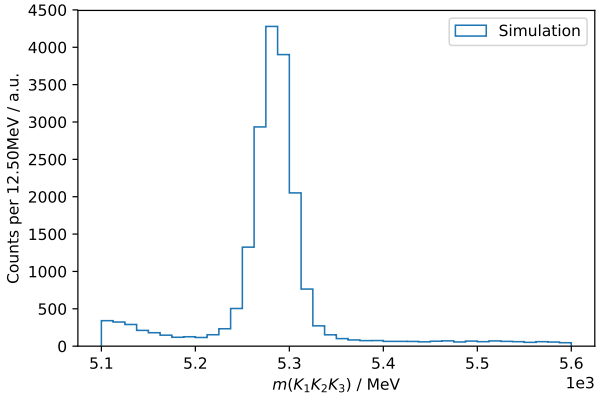

Figure 4: Invariant mass distribution of the $B^{\pm}$.

To calculate the global CP-asymmetry A_{CP} the signal counts of the B^{+} and B^{-} have to be determined. This is achieved by fitting the function

$$f(x) = B\exp\left(-\lambda x\right) + A\exp\left(\frac{(x-\mu)^2}{2\sigma^2}\right) \tag{7}$$

on the counts determined from a histogram and calculating the signal counts as the area under the Gaussian function $N = \sqrt{2\pi}A\sigma$. The plots of the fitted data for both B^{+} and B^{-} candidates are given Figure 5

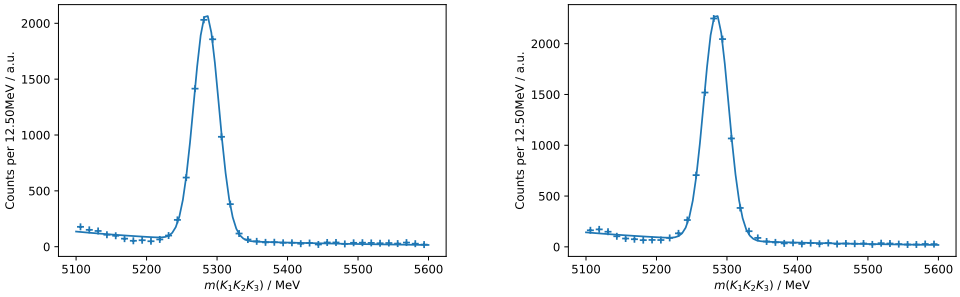

(a) B^+ **(b)** B^-

Figure 5: Function Equation 7 fitted on the counts determined from the histograms of both B^+ and B^- candidates.

The determined signal counts are used to calculate the global asymmetry factor A_{glo} using (1). The global asymmetry factor equates to

$$A_{\text{glo}} = 0.044\,69 \pm 0.008\,15 \tag{8}$$

with a significance of $S = 5.48$, where (3) and (4) are used to calculate the error and significance of the asymmetry, respectively.

Next, Dalitz plots are created to remove different resonances from the data samples. For the Dalitz plot, each possible invariant mass of the combination of two of the three Kaons is created. The two possible resonances, where the sum of the charges is zero are then used to create the Dalitz plot. The Dalitz plots of the simulation sample and the data sample in Figure 6.

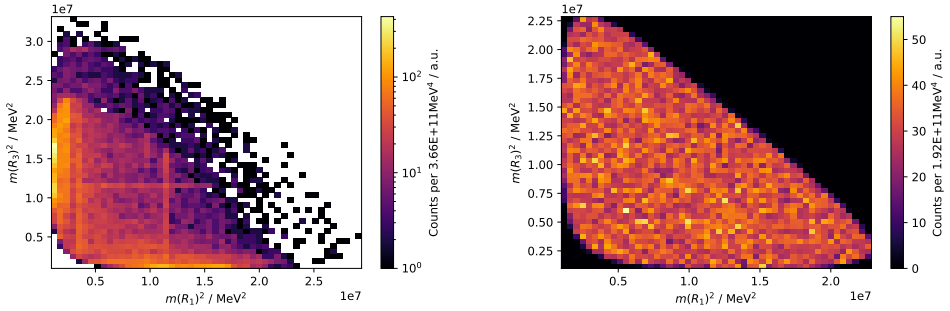

(a) Data sample **(b)** Simulation sample

Figure 6: Dalitz plot of the simulation sample (6b) and the data sample (6a).

Another way of creating a Dalitz plot is to compare the masses of the resonances and plot the lower mass on one and the higher mass on the other axis, as seen in Figure 7a. Recreating the same plot again as a scatter plot instead of a two-dimensional histogram improves the visibility of the resonances, as shown in Figure 7b.

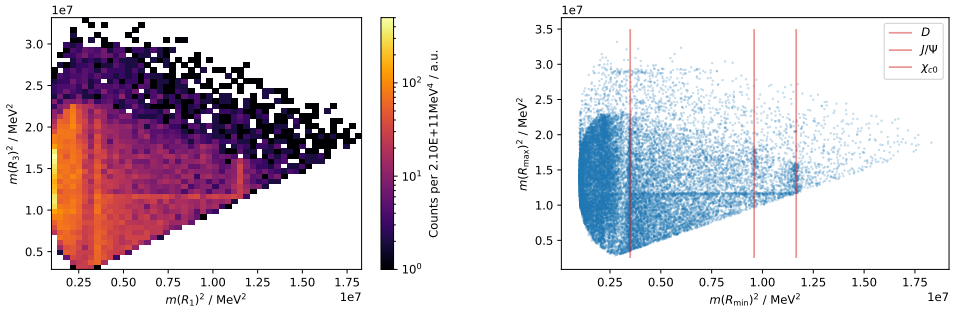

(a) Alternative Dalitz plot with $R_{\min}$ and $R_{\max}$.

(b) Scatter plot of the resonance masses squared of the data sample.

In the second plot, the resonances can be identified much easier. The unwanted resonances are identified as the D-meson, J-ψ, and the χ_{c0} and then removed by applying another requirement. This requirement is determined by removing the candidates where the R_1 and R_3 mass are in the range of 20 MeV close to the nominal masses of the D-meson, J-ψ or the χ_{c0}.

Lastly, the local asymmetry is determined. This is achieved by obtaining the counts in a given energy range. The counts of B^+ and B^- are determined respectively by creating two two-dimensional histograms, shown in Figure 8.

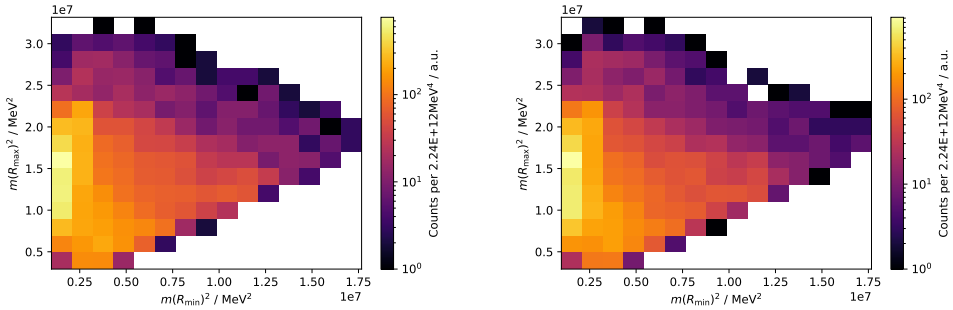

(a) B^-

(b) B^+

Figure 8: Two dimensional histograms of the B^+ and B^-.

The counts obtained by these plots are used to calculate a "per-bin" asymmetry factor, as seen in Figure 9a. Additionally, the significance of each bin is determined and shown in Figure 9b.

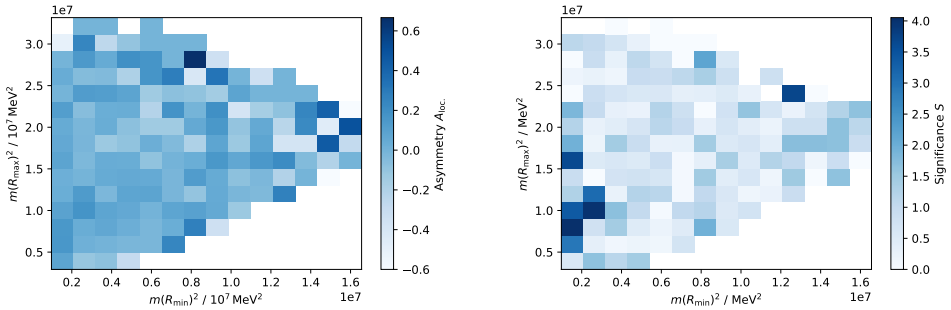

(a) Determined "per-bin" CP asymmetry factor.

(b) Local significance of the calculated CP asymmetry.

The energy region with a high CP asymmetry is chosen as:

$$0.98 \times 10^6\,\text{MeV}^2 < m(R_{\text{max}})^2 < 4.32 \times 10^6\,\text{MeV}^2$$
$$2.92 \times 10^6\,\text{MeV}^2 < m(R_{\text{min}})^2 < 21.07 \times 10^6\,\text{MeV}^2$$

The candidates in this region are used to determine the CP asymmetry factor via the aforementioned fit method. Additionally, the invariant mass distribution of the candidates is histogrammed in Figure 10 to visualize this asymmetry.

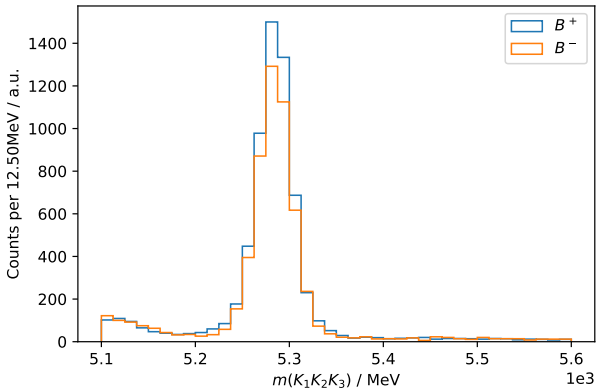

Figure 10: Invariant mass distribution of the B^+ and B^- in the high CP asymmetry region.

From the fits mentioned above the local CP asymmetry factor

$$A_{\text{loc}} = 0.062\,86 \pm 0.010\,17 \tag{9}$$

is calculated, with a resulting significance of $S = 6.18$.

6 Discussion

Looking at the requirements placed `prob` variables of the data were left untouched as lowering the background in Figure 5 would not allow for a good fit on the background distribution.

The distribution obtained from the invariant mass resembles the expected one, meaning an exponential function for the background and a Gaussian bell curve for the signal candidates. These functions were then fitted onto the data. From these fits the global asymmetry factor $A_{\text{glo}} = 0.044\,69 \pm 0.008\,15$ obtained with a significance of $S = 5.48$. This result fulfills the $5\,\sigma$ requirement placed on claiming a n observation of CP violation.

The Dalitz plots of both the simulation sample as well as the data sample also meet the expectation. For the simulation sample, the Dalitz plot looks mostly homogeneously, whereas the Dalitz plot obtained from the data sample shows the expected symmetry as well as some lines from certain resonances determined in the section above. These resonances become more visible in the alternative Dalitz plot shown in Figure 7a. The resonances were then removed from the data allowing for a cleaner data sample.

The last part of the analysis was the determination of the local asymmetry factor $A_{\text{loc}} = 0.062\,86 \pm 0.010\,17$ with a significance of $S = 6.18$. This significance is even higher than the one calculated for the global asymmetry. Even the asymmetry factor A_{loc} of the candidates in the determined high significance area was larger. This may result from the removal of the resonances, which do not contribute to the asymmetry.

All in all, it can be said that the analysis was able to produce good results with both the local and global asymmetry factor calculation resulting in a significance > 5.

References

[1] J. Beringer et al. “Review of Particle Physics (RPP)”. In: *Phys.Rev.* (2012). DOI: 10.1103/PhysRevD.86.010001.

[2] Makoto Kobayashi and Toshihide Maskawa. “CP-Violation in the Renormalizable Theory of Weak Interaction”. In: *Progress of Theoretical Physics* 49.2 (Feb. 1973), pp. 652–657. DOI: 10.1143/PTP.49.652. URL: https://doi.org/10.1143/PTP.49.652.

[3] *Measurement of matter-antimatter asymmetries with the LHCb experiment*. TU Dortmund, Department of physics.